

Jeremiah Y. Cohen, Pierre Pouget, Richard P. Heitz, Geoffrey F. Woodman and Jeffrey D. Schall

J Neurophysiol 101:912-916, 2009. First published Dec 3, 2008; doi:10.1152/jn.90272.2008

You might find this additional information useful...

This article cites 40 articles, 31 of which you can access free at:

<http://jn.physiology.org/cgi/content/full/101/2/912#BIBL>

Updated information and services including high-resolution figures, can be found at:

<http://jn.physiology.org/cgi/content/full/101/2/912>

Additional material and information about *Journal of Neurophysiology* can be found at:

<http://www.the-aps.org/publications/jn>

This information is current as of February 28, 2009 .

Biophysical Support for Functionally Distinct Cell Types in the Frontal Eye Field

Jeremiah Y. Cohen, Pierre Pouget, Richard P. Heitz, Geoffrey F. Woodman, and Jeffrey D. Schall

Department of Psychology, Vanderbilt Brain Institute, Center for Integrative and Cognitive Neuroscience, Vanderbilt Vision Research Center, Vanderbilt University, Nashville, Tennessee

Submitted 15 February 2008; accepted in final form 28 November 2008

Cohen JY, Pouget P, Heitz RP, Woodman GF, Schall JD. Biophysical support for functionally distinct cell types in the frontal eye field. *J Neurophysiol* 101: 912–916, 2009. First published December 3, 2008; doi:10.1152/jn.90272.2008. Numerous studies have described different functional cell types in the frontal eye field (FEF), but the reliability of the distinction between these types has been uncertain. Studies in other brain areas have described specific differences in the width of action potentials recorded from different cell types. To substantiate the functionally defined cell types encountered in FEF, we measured the width of spikes of visual, movement, and visuomovement types of FEF neurons in macaque monkeys. We show that visuomovement neurons had the thinnest spikes, consistent with a role in local processing. Movement neurons had the widest spikes, consistent with their role in sending eye movement commands to subcortical structures such as the superior colliculus. Visual neurons had wider spikes than visuomovement neurons, consistent with their role in receiving projections from occipital and parietal cortex. These results show how structure and function of FEF can be linked to guide inferences about neuronal architecture.

INTRODUCTION

This paper concerns the general problem of how the primate brain transforms visual input into eye-movement output. Several cortical areas and subcortical regions contribute to this visual-motor mapping. One such area, the frontal eye field (FEF), contains at least three main functional types of neurons: visual, movement, and visuomovement neurons (Bruce and Goldberg 1985; DiCarlo and Maunsell 2005; Goldberg and Bushnell 1981; Hanes et al. 1998; Kodaka et al. 1997; Schall 1991; Segraves 1992; Segraves and Goldberg 1987; Umeno and Goldberg 1997). In FEF, a population of visual and visuomovement neurons selects the target of search by increasing their firing rate in response to the presence of the target in their receptive fields (RFs) relative to when a distractor is situated in their RFs (e.g., Schall and Hanes 1993; Thompson et al. 1996). A different population of neurons, called movement neurons, increases their firing rate leading up to saccades into their movement fields (MFs) (e.g., Hanes and Schall 1996). Visuomovement neurons also increase their firing rate leading up to saccades. Despite these differences, distinctions between these cell types have relied largely on firing-rate patterns as opposed to inherent biophysical properties of the neurons being studied. Moreover, disagreements persist about the reliability of the distinction between cell types.

Understanding how visuomotor transformations occur requires knowledge of the underlying circuitry, which is composed of different types of neurons. Cortical neurons have been distinguished by morphology (Kawaguchi 1995; Krimer et al. 2005), neurotransmitter (Connors and Gutnick 1990), laminar distribution (Bullier and Henry 1979; Condé et al. 1994; Dow 1974), molecular composition (Cauli et al. 1997; Martina et al. 1998), functional property (González-Burgos et al. 2005), and developmental origin (Letinic et al. 2002). Differences between neuron types have typically been distinguished in vitro or intracellularly. Several studies, however, have distinguished types of neurons by the shape of extracellularly recorded action potentials (Barthó et al. 2004; Chen et al. 2008; Constantinidis and Goldman-Rakic 2002; Csicsvari et al. 1999; Henze et al. 2000; Mountcastle et al. 1969). For example, extracellular recordings of neurons in extrastriate visual cortex (V4) have shown that neurons with thin spikes (putative interneurons) showed stronger attentional modulation than neurons with wider spikes (Mitchell et al. 2007).

To determine whether functional cell types in FEF exhibit biophysical differences, we measured spike waveforms of functional cell types distinguished by their responses following visual stimuli or before saccades. The results are consistent with the hypothesis that different functional cell types correspond to different anatomical cell types.

METHODS

Behavioral task and recording

All experimental procedures were performed in accordance with the National Institutes of Health Guide for the Care and Use of Laboratory Animals and approved by the Vanderbilt Institutional Animal Care and Use Committee. Activity of FEF neurons was recorded in four male macaques (*Macaca radiata*) performing three different tasks that have been described in detail previously. *Monkey Q* performed visual search for a singleton target defined by color (Cohen et al. 2007; Sato et al. 2001). *Monkeys Q* and *S* performed visual search for a target (T or L) among distractors (Ls or Ts, respectively) (Woodman et al. 2007). *Monkeys M* and *U* performed a saccade stop signal (countermanding) task (Hanes et al. 1998). All monkeys were trained on a memory-guided saccade task. Activity from each neuron was recorded during this task to distinguish visual- from movement-related activity (Bruce and Goldberg 1985; Hikosaka and Wurtz 1983).

Address for reprint requests and other correspondence: J. D. Schall, 111 21st Ave. South, Nashville, TN 37203 (E-mail: jeffrey.d.schall@vanderbilt.edu).

Our data set consists of 12 neurons from *monkey Q* during the color singleton visual search task, 48 neurons from *monkey Q* during the form visual search task, 20 neurons from *monkey S* during the form visual search task, 9 neurons from *monkey M* during the countermanding task, and 5 neurons from *monkey U* during the countermanding task, for a total of 94 neurons. Spikes were sorted on-line and off-line using principal components analysis (Plexon). A neuron was only considered for analysis if its spike waveforms were clearly discriminable and its activity was clearly visual related, movement related, or visual and movement related.

Data analysis

To measure the firing rate of each neuron, we used a spike density function, convolving each spike with a kernel resembling a postsynaptic potential (Thompson et al. 1996). We used the memory-guided saccade task to classify neurons. Visual neurons had significantly greater activity in the 100 ms after the target flash than in the 100 ms before the target flash. Movement neurons had greater responses in the 100 ms leading up to the saccade than in the 100 ms before the target flash. Visuomovement neurons had greater responses in the 100 ms after the target flash and in the 100 ms leading up to the saccade than in the 100 ms before the target flash.

Because spike amplitude, but not width, is dependent on the distance from electrode tip (Henze et al. 2000), we used spike width as a measure of action potential shape. We applied a smoothing spline to each mean spike waveform. Spike width was computed as the time from trough to peak (Mitchell et al. 2007) (see Fig. 2A). This measure resulted in smaller spike width values than those reported in other studies (e.g., Constantinidis and Goldman-Rakic 2002), which measured spike width as the time from first to second trough. Spike waveforms were sampled at 40 kHz for 800 μ s.

In addition to classifying neurons based on their activity during the memory-guided saccade task, we computed a visuomovement index for each neuron based on activity during the search or countermanding task in the RF location that elicited the largest response during the memory-guided task. The index was computed as $(V - B)/(M - B)$, where V is the neuron's average visual-related firing rate from 50 to 150 ms after target onset, M is its average movement-related firing rate from 100 ms before saccades to the time of saccades and B is its average baseline firing rate 100 ms before target onset. We did not use spike density functions to compute visuomovement indices.

We measured spiking variability using the coefficient of variation (CV) (Softky and Koch 1993) in bins of 100 interspike intervals. The CV is defined as the ratio of the SD to the mean of the interspike intervals.

To measure differences between groups of neurons, we used Wilcoxon rank sum tests with Bonferroni corrections for multiple comparisons. All analyses were performed in R (R Development Core Team 2008).

RESULTS

We analyzed the activity of 94 FEF neurons from four monkeys during memory-guided visual search and countermanding tasks. We classified neurons as visual, movement or visuomovement and compared spike widths across functionally defined neuron types.

Types of FEF neurons

To classify neurons, we measured responses during the memory-guided saccade task. We classified 33 neurons as visual,

28 as movement, and 33 as visuomovement. The fraction of visuomovement neurons is lower than reported in previous studies (Bruce and Goldberg 1985; Schall 1991). Figure 1 shows average firing rates for a representative neuron of each type during the memory-guided task. Figure 1A, *left*, shows the firing rate of a visual neuron aligned to target onset. The neuron had its largest response following the target flash in its RF (cumulative distribution of saccade times shown as dashed gray curve). Figure 1A, *right*, shows the firing rate of the same neuron aligned to the time of saccade (dashed line). The neuron did not fire above baseline prior to saccades. Figure 1B shows the response of a movement neuron. This neuron increased its firing rate leading up to saccades (*right*). It did not fire above baseline in response to the target flash (*left*). Figure 1C shows the response of a visuomovement neuron. This neuron responded to the visual stimulus and before saccades. We found no difference in spike amplitude or firing rate between types of neurons.

Spike widths

After categorizing neurons, we measured the width of the mean spike waveform for each neuron from trough to peak (Fig. 2). Figure 2A shows an example mean spike waveform from a visuomovement neuron and demonstrates our method

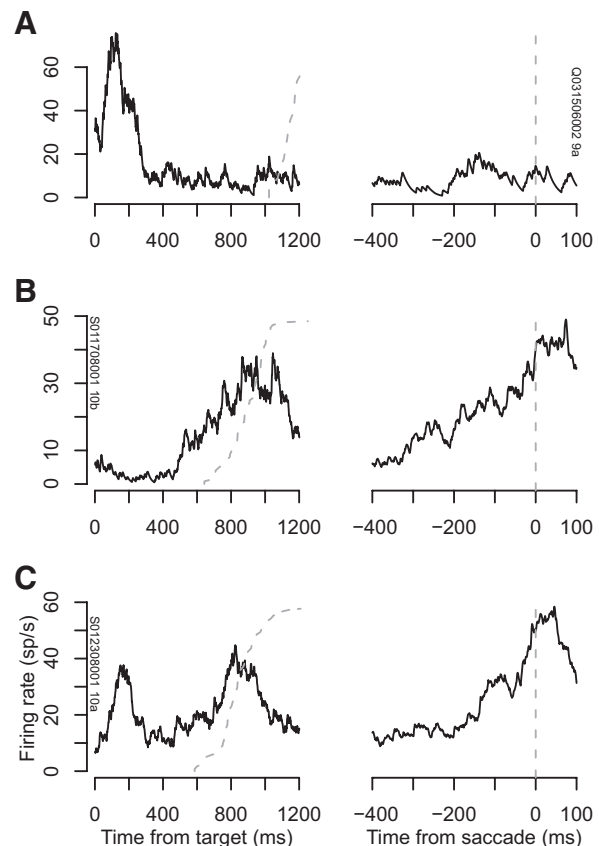


FIG. 1. Representative visual (A), movement (B), and visuomovement (C) neurons. *Left*: average firing rate during the memory-guided saccade task aligned to the time of presentation of the target inside the neuron's receptive field. Dashed gray line plots the distribution of response times. *Right*: average firing rate aligned on the time of saccade initiation (dashed gray line).

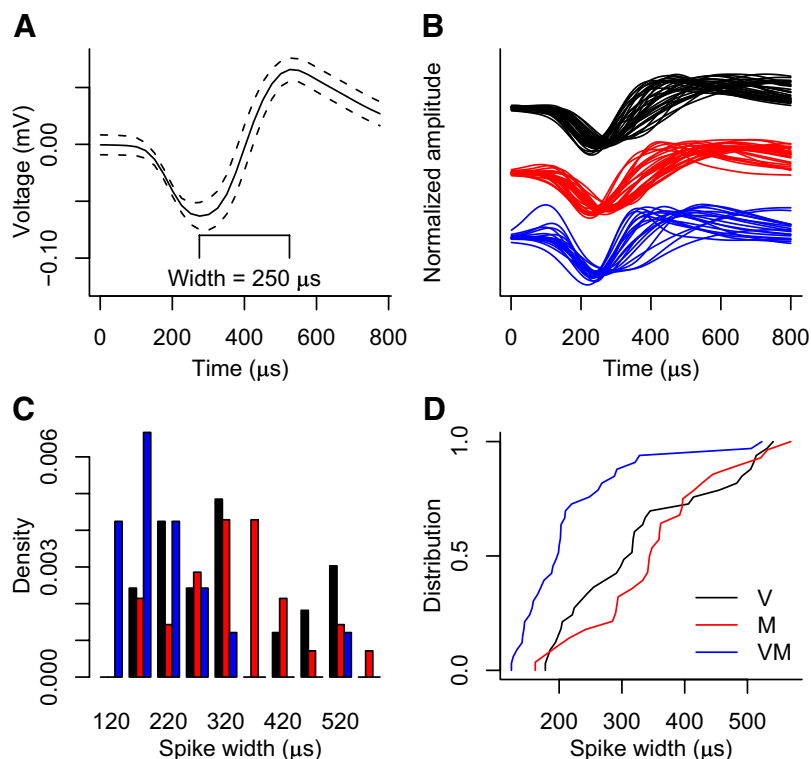


FIG. 2. Spike width by neuron type. A: mean (—) and mean \pm SD (---) spike waveforms from a representative visuomovement neuron. B: all mean, normalized spike waveforms for visual (V, black), movement (M, red) and visuomovement (VM, blue) neurons. C: histogram of spike widths for each type of neuron. D: cumulative distribution of spike widths for each type of neuron.

for computing spike width. This neuron had a mean spike width of 250 μ s. Figure 2B shows all the normalized mean spike waveforms for visual neurons (black), movement neurons (red) and visuomovement neurons (blue) fitted with smoothing splines. Each mean spike waveform was normalized by dividing its values by the difference of its maximum and minimum values. Figure 2C shows histograms of spike widths of all neurons of each type, and Fig. 2D shows the cumulative distributions of spike widths for each type of neuron. The mean spike widths (\pm SE) were 329 \pm 20.5 μ s for visual neurons (V), 352 \pm 19.5 μ s for movement neurons (M), and 218 \pm 16.4 μ s for visuomovement neurons (VM).

A Kruskal-Wallis rank sum test revealed a significant effect of neuron type ($\chi^2 = 28.1$, $P < 0.001$). Spike widths were significantly larger for movement neurons than for visuomovement neurons (Wilcoxon rank sum test with Bonferroni correction for multiple comparisons, $P < 0.001$) and larger for visual neurons than for visuomovement neurons ($P < 0.005$). There was no significant difference between visual and movement neuron spike widths ($P > 0.3$).

To verify that the demands of the task did not affect the shape of a neuron's spike, we compared the spike widths during the intertrial intervals and during the period from target onset to saccade onset. All neurons showed no difference in spike width between task performance and baseline activity ($P > 0.9$).

We computed a visuomovement index for each neuron defined as the ratio of the difference between visual activity and baseline activity and movement activity and baseline activity during the search or countermanding task. Classifying neurons using the visuomovement index reproduced classification using the activity during the memory-guided task. Figure 3A shows boxplots of visuomovement indices grouped by neuron type as defined in the memory-guided task. Visuomovement

indices were significantly different between visual and movement neurons (Wilcoxon rank sum test with Bonferroni correction for multiple comparisons, $P < 0.001$), between visual and visuomovement neurons ($P < 0.001$) and between movement and visuomovement neurons ($P < 0.001$). To obtain an independent classification of neurons, we divided the distribution of visuomovement indices into three groups. Figure 3B shows this division and the classification of neurons into visual (V), movement (M), and visuomovement (VM) categories. Two visuomovement neurons were classified differently using the visuomovement index, one as a visual neuron and one as a movement neuron. These are shown as gray points in Fig. 3B. Using this classification, spike widths were significantly larger for visual than visuomovement neurons ($P < 0.001$) and for movement than visuomovement neurons ($P < 0.001$). There was no significant difference in spike width between visual and movement neurons ($P > 0.7$).

Neuron classification using the visuomovement index was robust within a small range of boundaries between classes of neurons. Figure 3, C and D, show the number of misclassified neurons as a function of the boundary between movement and visuomovement neurons and visuomovement and visual neurons for each type of neuron. The boundaries shown in Fig. 3B (0.2 and 0.7) correspond to the minimum number of misclassified neurons (the 2 visuomovement neurons shown in gray in Fig. 3B). These boundaries are indicated by dashed vertical lines in Fig. 3, C and D.

Spiking variability

To obtain another measure useful for distinguishing neuron types, we measured the coefficient of variation of spiking (CV) in bins of 100 interspike intervals. Figure 4 shows cumulative distributions of CV for the three classes of neurons. CV was

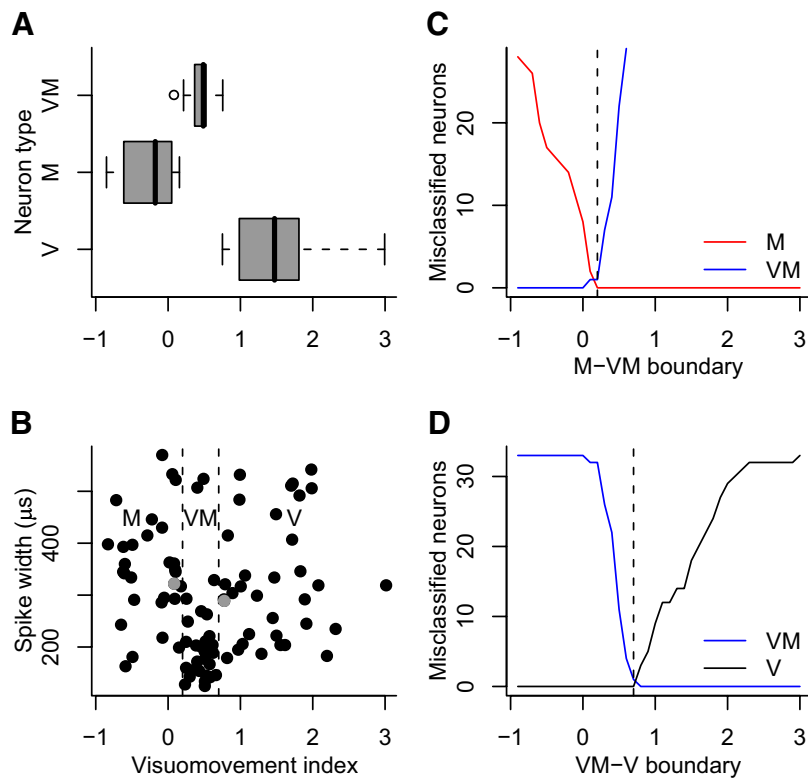


FIG. 3. Visuomovement index. *A*: boxplot of visuomovement indices derived from activity during the memory-guided saccade task. *B*: scatter plot of spike width vs. visuomovement index. Neurons were classified into movement (*M*), visuomovement (*VM*), and visual (*V*) groups separated by dashed black lines, and 2 neurons that were classified as visuomovement during the memory-guided task were classified differently using the index; these are shown in gray. *C*: number of misclassified *M* and *VM* neurons as a function of the boundary between *M* and *VM* in *B*. The value minimizing the number of misclassified neurons was 0.2, indicated by the dashed vertical line. *D*: number of misclassified *VM* and *V* neurons as a function of the boundary between *VM* and *V* in *B*. The value minimizing the number of misclassified neurons was 0.7, indicated by the dashed vertical line.

significantly larger for visuomovement neurons than for visual neurons (Wilcoxon rank sum test, $P < 0.001$) and for movement neurons ($P < 0.001$). CV was not significantly different between visual and movement neurons (Wilcoxon rank sum test, $P > 0.5$).

DISCUSSION

We have shown that three functional types of FEF neurons have different spike waveforms. This suggests that distinct types of neurons defined functionally may constitute different types of neurons defined morphologically. It is tempting to

classify visuomovement neurons, those neurons with the thinnest spikes, as local inhibitory interneurons. We cannot, however, say that all neurons with short spike durations are inhibitory. Some studies suggest only particular subclasses of GABAergic neurons display short spike durations (McCormick et al. 1985; Naegel and Katz 1990). Some or all may be small neurons with local excitatory connections (Gur et al. 1999). Likewise, we cannot say that all visual and movement neurons are pyramidal neurons because they have wider spikes than visuomovement neurons although data from anatomical and physiological studies are in agreement with such a claim (Fries 1984; Seigraves and Goldberg 1987; Sommer and Wurtz 1998, 2001).

Are there really three categories of neurons in FEF? Although there appears to be a continuum of responses from visual related to movement related (see Fig. 3), our results reveal a significant difference in spike width related to functional neuron classification. This is important for exposing the possibility that visuomovement neurons may constitute a different morphological type of neuron than visual or movement neurons. While further research is needed to verify or refute this hypothesis, the current results add to a growing literature providing evidence for the heterogeneity of neurons in FEF. The ability to distinguish types of neurons in FEF is necessary to understand whether the visual to motor transformation occurs within or across distinct neuron types.

GRANTS

This work was supported by National Institutes of Health Grants T32-MH-064913, R01-EY-08890, P30-EY-08126, and P30-HD-015052, the McKnight Endowment Fund for Neuroscience, and Robin and Richard Patton through the E. Bronson Ingram Chair in Neuroscience.

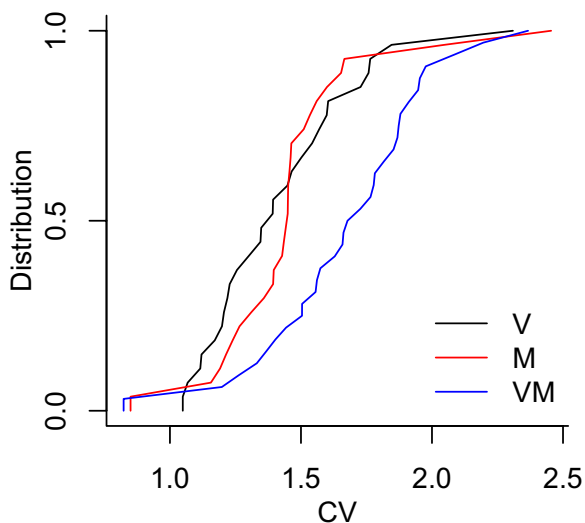


FIG. 4. Cumulative distributions of CV in bins of 100 ISIs for visual (*V*), movement (*M*), and visuomovement (*VM*) neurons.

REFERENCES

- Barthó P, Hirase H, Monconduit L, Zugaro M, Harris KD, Buzsáki G.** Characterization of neocortical principal cells and interneurons by network interactions and extracellular features. *J Neurophysiol* 92: 600–608, 2004.
- Bruce CJ, Goldberg ME.** Primate frontal eye fields. I. Single neurons discharging before saccades. *J Neurophysiol* 53: 603–635, 1985.
- Bullier J, Henry GH.** Laminar distribution of first-order neurons and afferent terminals in cat striate cortex. *J Neurophysiol* 42: 1271–1281, 1979.
- Cauli B, Audinat E, Lambollez B, Angulo MC, Ropert N, Tsuzuki K, Hestrin S, Rossier J.** Molecular and physiological diversity of cortical nonpyramidal cells. *J Neurosci* 17: 3894–3906, 1997.
- Chen Y, Martínez-Conde S, Macknik SL, Bereshpolova Y, Swadlow HA, Alonso, JM.** Task difficulty modulates the activity of specific neuronal populations in primary visual cortex. *Nat Neurosci* 11: 974–982, 2008.
- Cohen JY, Pouget P, Woodman GF, Subraveti CR, Schall JD, Rossi AF.** Difficulty of visual search modulates neuronal interactions and response variability in the frontal eye field. *J Neurophysiol* 98: 2580–2587, 2007.
- Condé F, Lund JS, Jacobowitz DM, Baimbridge KG, Lewis DA.** Local circuit neurons immunoreactive for calretinin, calbindin D-28k or parvalbumin in monkey prefrontal cortex: distribution and morphology. *J Comp Neurol* 341: 95–116, 1994.
- Connors BW, Gutnick MJ.** Intrinsic firing patterns of diverse neocortical neurons. *Trends Neurosci* 13: 99–104, 1990.
- Constantinidis C, Goldman-Rakic PS.** Correlated discharges among putative pyramidal neurons and interneurons in the primate prefrontal cortex. *J Neurophysiol* 88: 3487–3497, 2002.
- Csicsvari J, Hirase H, Czurkó A, Mamiya A, Buzsáki G.** Oscillatory coupling of hippocampal pyramidal cells and interneurons in the behaving rat. *J Neurosci* 19: 274–287, 1999.
- DiCarlo JJ, Maunsell JH.** Using neuronal latency to determine sensory-motor processing pathways in reaction time tasks. *J Neurophysiol* 93: 2974–2986, 2005.
- Dow BM.** Functional classes of cells and their laminar distribution in monkey visual cortex. *J Neurophysiol* 37: 927–946, 1974.
- Fries W.** Cortical projections to the superior colliculus in the macaque monkey: a retrograde study using horseradish peroxidase. *J Comp Neurol* 230: 55–76, 1984.
- Goldberg ME, Bushnell MC.** Behavioral enhancement of visual responses in monkey cerebral cortex. II. Modulation in frontal eye fields specifically related to saccades. *J Neurophysiol* 46: 773–787, 1981.
- González-Burgos G, Krimer LS, Povysheva NV, Barrionuevo G, Lewis DA.** Functional properties of fast spiking interneurons and their synaptic connections with pyramidal cells in primate dorsolateral prefrontal cortex. *J Neurophysiol* 93: 942–953, 2005.
- Gur M, Beylin A, Snodderly DM.** Physiological properties of macaque V1 neurons are correlated with extracellular spike amplitude, duration, and polarity. *J Neurophysiol* 82: 1451–1464, 1999.
- Hanes DP, Patterson WF, Schall JD.** Role of frontal eye fields in countermanding saccades: visual, movement, and fixation activity. *J Neurophysiol* 79: 817–834, 1998.
- Hanes DP, Schall JD.** Neural control of voluntary movement initiation. *Science* 274: 427–430, 1996.
- Henze DA, Borhegyi Z, Csicsvari J, Mamiya A, Harris KD, Buzsáki G.** Intracellular features predicted by extracellular recordings in the hippocampus in vivo. *J Neurophysiol* 84: 390–400, 2000.
- Hikosaka O, Wurtz RH.** Visual and oculomotor functions of monkey substantia nigra pars reticulata. III. Memory-contingent visual and saccade responses. *J Neurophysiol* 49: 1268–1284, 1983.
- Kawaguchi Y.** Physiological subgroups of nonpyramidal cells with specific morphological characteristics in layer II/III of rat frontal cortex. *J Neurosci* 15: 2638–2655, 1995.
- Kodaka Y, Mikami A, Kubota K.** Neuronal activity in the frontal eye field of the monkey is modulated while attention is focused on to a stimulus in the peripheral visual field, irrespective of eye movement. *Neurosci Res* 28: 291–298, 1997.
- Krimer LS, Zaitsev AV, Czanner G, Kröner S, González-Burgos G, Povysheva NV, Iyengar S, Barrionuevo G, Lewis DA.** Cluster analysis-based physiological classification and morphological properties of inhibitory neurons in layers 2–3 of monkey dorsolateral prefrontal cortex. *J Neurophysiol* 94: 3009–3022, 2005.
- Leticic K, Zoncu R, Rakic P.** Origin of GABAergic neurons in the human neocortex. *Nature* 417: 645–649, 2002.
- Martina M, Schultz JH, Ehmke H, Monyer H, Jonas P.** Functional and molecular differences between voltage-gated K⁺ channels of fast-spiking interneurons and pyramidal neurons of rat hippocampus. *J Neurosci* 18: 8111–8125, 1998.
- McCormick DA, Connors BW, Lighthall JW, Prince DA.** Comparative electrophysiology of pyramidal and sparsely spiny stellate neurons of the neocortex. *J Neurophysiol* 54: 782–806, 1985.
- Mitchell JF, Sundberg KA, Reynolds JH.** Differential attention-dependent response modulation across cell classes in macaque visual area V4. *Neuron* 55: 131–141, 2007.
- Mountcastle VB, Talbot WH, Sakata H, Hyvärinen J.** Cortical neuronal mechanisms in utter-vibration studied in unanesthetized monkeys. Neuronal periodicity and frequency discrimination. *J Neurophysiol* 32: 452–484, 1969.
- Naegele JR, Katz LC.** Cell surface molecules containing N-acetyl-galactosamine are associated with basket cells and neurogliaform cells in cat visual cortex. *J Neurosci* 10: 540–557, 1990.
- R Development Core Team.** *R: A Language and Environment for Statistical Computing*. Vienna, Austria: R Foundation for Statistical Computing, 2008.
- Sato T, Murthy A, Thompson KG, Schall JD.** Search efficiency but not response interference affects visual selection in frontal eye field. *Neuron* 30: 583–591, 2001.
- Schall JD.** Neuronal activity related to visually guided saccades in the frontal eye fields of rhesus monkeys: comparison with supplementary eye fields. *J Neurophysiol* 66: 559–579, 1991.
- Schall JD, Hanes DP.** Neural basis of saccade target selection in frontal eye field during visual search. *Nature* 366: 467–469, 1993.
- Segraves MA.** Activity of monkey frontal eye field neurons projecting to oculomotor regions of the pons. *J Neurophysiol* 68: 1967–1985, 1992.
- Segraves MA, Goldberg ME.** Functional properties of corticotectal neurons in the monkey's frontal eye field. *J Neurophysiol* 58: 1387–1419, 1987.
- Softky WR, Koch C.** The highly irregular firing of cortical cells is inconsistent with temporal integration of random EPSPs. *J Neurosci* 13: 334–350, 1993.
- Sommer MA, Wurtz RH.** Frontal eye field neurons orthodromically activated from the superior colliculus. *J Neurophysiol* 80: 3331–3335, 1998.
- Sommer MA, Wurtz RH.** Frontal eye field sends delay activity related to movement, memory, and vision to the superior colliculus. *J Neurophysiol* 85: 1673–1685, 2001.
- Thompson KG, Hanes DP, Bichot NP, Schall JD.** Perceptual and motor processing stages identified in the activity of macaque frontal eye field neurons during visual search. *J Neurophysiol* 76: 4040–4055, 1996.
- Umeno MM, Goldberg ME.** Spatial processing in the monkey frontal eye field. I. Predictive visual responses. *J Neurophysiol* 78: 1373–1383, 1997.
- Woodman GF, Kang M-S, Rossi AF, Schall JD.** Nonhuman primate event-related potentials indexing covert shifts of attention. *Proc Natl Acad Sci USA* 104: 15111–15116, 2007.